Layered Molecular Ordering of Self-Organized Poly(3-hexylthiophene) Thin Films on Hydrophobized Surfaces

Do Hwan Kim, Yunseok Jang, Yeong Don Park, and Kilwon Cho*

Department of Chemical Engineering/Polymer Research Institute, Pohang University of Science and Technology, Pohang 790-784, Korea

Received February 27, 2006; Revised Manuscript Received June 20, 2006

ABSTRACT: In this study, we used cross-sectional transmission electron microscopy to directly visualize the internal structure of regioregular poly(3-hexylthiophene) (P3HT) on hydrophobized insulator substrates. By examining the variation in the electron contrasts, we found that these P3HT films are self-organized with layered molecular ordering. Further, by analyzing grazing incidence-angle X-ray diffraction results, we found that highly oriented, nanoscopic domains composed of P3HT chains with face-on orientations are present.

Introduction

π-Conjugated polymers are regarded as one of the most promising materials for use in so-called plastic electronics because of their excellent electrical and optical properties,[1] reasonable chemical stability, and easy processability.[2] In particular, poly(3-hexylthiophene) (P3HT) belongs to this important class of conjugated polymers. Regioregular P3HT has been used as the active material in organic field-effect transistors (OFETs),[3] in which the preferential supramolecular ordering of the polymer chains produces a high charge carrier mobility of up to 0.1 $cm^2\ V^{-1}\ s^{-1}$, approaching that of single-crystal oligothiophenes.[2a,3a,c,h,4]

Further, self-organized regioregular P3HT with its supramolecular two-dimensional structure is of special interest because the one-dimensional electronic properties of the π-conjugated polymer chains are modified by the interchain stacking that results from their $\pi-\pi$ interactions.[3,5] A number of external factors can affect the degree of ordering in the lamellar structure of the nanocrystalline regions in such films. To enhance the two-dimensional molecular ordering of π-conjugated polymer films, many groups have examined the outcomes of modifying the molecular parameters (regioregularity,[3c,6a] molecular weight,[6b−d] and side-chain length[6e,f]) and processing conditions (solvent power,[2a,6g] film thickness,[6h] doping level,[6i] and film forming method[6j−l]). In a previous study,[7a] we found that in an ~70 nm thick film, depending on the surface characteristics of the insulator substrate, the P3HT nanocrystals adopt two different orientations—parallel and perpendicular to the insulator substrate—which have field-effect mobilities that differ by more than a factor of 4 and that are as high as 0.28 $cm^2\ V^{-1}\ s^{-1}$. This surprisingly high field-effect mobility arises in particular for the perpendicular orientation (edge-on structure) of the nanocrystals with respect to an insulator substrate treated with a self-assembled monolayer (SAM) with $-NH_2$ functional group. Many groups have also studied the surface morphologies of, and chain orientations in, P3HT thin films spin-coated on insulator substrates hydrophobized with hexamethyldisilazane (HMDS) and octadecyltrichlorosilane (ODTS), which have $-CH_3$ functional groups. In particular, we found that the face-on orientation arises for hydrophobized insulator substrates as a result of carrying out the annealing process above the melting temperature (~240 °C), irrespective of whether the deposited layer is a thick film[7a] or monolayer system.[7b] It has been shown that P3HT films grown on HMDS-coated substrates (hydrophobized surfaces) have edge-on or face-on orientations depending on the P3HT regioregularity[3c] and that the tuning of P3HT film morphology and chain orientation can be achieved by varying the molecular weight[6b,c] and the solvent.[6d] However, none of these samples were annealed above the melting temperature of P3HT after spin-coating. It should be a dynamic phenomenon, i.e., thermodynamically nonequilibrium state, during the rapid growth of spin-coated films although the solvent with high-boiling temperature was selected. In contrast, we selected an annealing temperature (240 °C) above the melting temperature of P3HT ($T_m \sim 216$ °C)[6l] in order to ensure that there was sufficient mobility of the P3HT chains for ordering to occur, and this approach was found to result in a profound effect on the surface-induced ordering of the P3HT chains on hydrophobized insulator substrates. It should also be noted that residual stress resulting from the spin-coating process can be excluded by annealing at a high temperature.

Despite the resulting improvements in the field-effect mobility of regioregular P3HT grown on hydrophobized surfaces, little is known about how the interface between regioregular P3HT and the hydrophobized insulator substrate is stabilized or how the internal morphology of a self-organized P3HT film can be optimized with respect to the insulator substrates. Also, in a couple of our previous papers,[7] we did not directly demonstrate the layered molecular structure in P3HT thin film self-organized on a hydrophobized surface.

In this study, we present the first report of the direct visualization of the layered molecular ordering in P3HT films grown on hydrophobized insulator substrates. To visualize the internal structure, i.e., obtain a precise image of the P3HT ordering, we used the cross-sectional transmission electron microscopy (TEM) method, after carrying out a doping process. Further, we focus on controlling the structural ordering that results from the intermolecular interactions at the interface between regioregular P3HT and the insulator (SiO_x) with the aim of enhancing the two-dimensional molecular ordering of the P3HT thin films. To achieve this goal, we modified the insulator substrates with an octyltrichlorosilane (OTS) self-assembled monolayer (SAM).

* To whom all correspondence should be addressed. E-mail: kwcho@postech.ac.kr.

10.1021/ma060427b CCC: $33.50
Published on Web 07/29/2006

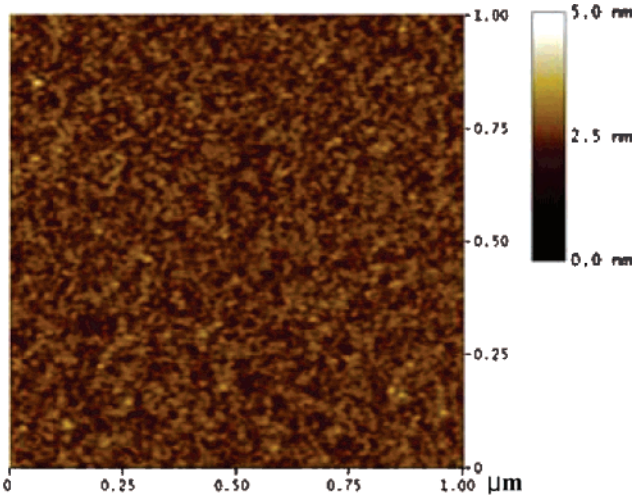

Figure 1. TM-AFM image (1 μm × 1 μm) of an OTS SAM with remarkable flatness (rms roughness ~ 2 Å) and uniformity.

Experimental Section

Sample Purification. The regioregular P3HT used in this study was obtained from Rieke Metals Inc. The molecular weight (M_n = 30 kg/mol, M_w = 54 kg/mol, M_w/M_n = 1.8) was determined by using size exclusion chromatography (SEC) relative to polystyrene (PS) standards.[7a] To obtain highly regioregular P3HT and narrow molecular weight distribution (as-received sample ~93%, M_w/M_n = 2.4), this polymer was purified by continuous extraction with THF and acetonitrile (HPLC grade, Duksan) due to the solubility difference between regiorandom and regioregular polymers.[6b,d,8] The regioregularity (98%) of our sample was estimated with ^{1}H NMR by comparing the intensities of the signals of 7.05, 7.03, 7.00, and 6.98 ppm that arise from the aromatic region of the spectrum.

Sample Preparation. The films were spin-coated from a 0.2 wt % solution in chloroform ($CHCl_3$) onto hydrophobized silicon substrates (Si/SiOx) modified with a CH_3-functionalized self-assembled monolayer (SAM) in order to change the surface characteristics and annealed at 240 °C under argon for 20 min followed by slow crystallization. To fabricate the SAM, we used octyltrichlorosilane (OTS) for $-CH_3$ end groups as silane coupling agents (Aldrich). To minimize the effects of the trace amounts of water in the surrounding atmosphere on the quality of the monolayers, the following procedures were carried out. The vacuum-dried reaction flasks were charged with anhydrous toluene and a piece of cleaned silicon substrate under argon. The silanes were then added to the flask (10 mM) and left to self-assemble on the substrates for 1 h under argon. Substrates modified with SAM were transferred to a 120 °C oven and baked for 20 min. Subsequently, the substrates were cleaned by ultrasonication in toluene and then dried under vacuum. We can observe that the self-assembled monolayer is well-defined from ellipsometer (8−9 Å), contact-angle measurements (104°), and tapping-mode atomic force microscopy (TM-AFM) data (Figure 1). As expected, OTS containing alkyl chain has the low surface energy, 26 mJ/m^2 (probe liquids: pure water and diiodomethane) and very flat surfaces (rms roughness ~ 2 Å). We also confirmed that the OTS−SAMs fabricated in this study were not deformed at 240 °C by using FT-IR, ellipsometry (8−9 Å), and contact-angle measurements (103°−104°).

Characterization Techniques. *Transmission Electron Microscopy.* To prepare each sample for cross-sectional TEM, a thin layer of carbon (~10 nm thick) was first evaporated onto the thin P3HT film grown on a hydrophobized silicon substrate, covered with an embedding epoxy (PolyBed 812 Kit, Polysciences, Inc.), and then cured at room temperature for 24 h and at 60 °C for 24 h. The epoxy/carbon/P3HT composite was peeled off from the silicon substrate by immersing the composite in liquid nitrogen. A thin layer of carbon was again evaporated onto the P3HT side of the detached composite and then covered with epoxy and cured as before. Thin sections (~40−50 nm thick) from the epoxy/carbon/P3HT/carbon/epoxy composite were obtained using an ultramicrotome with a diamond knife. The sectioned specimens were exposed to 1 wt % $ZnCl_2$ solution for 10 min. TEM was performed on a HITACHI-7600 operating at 120 kV.

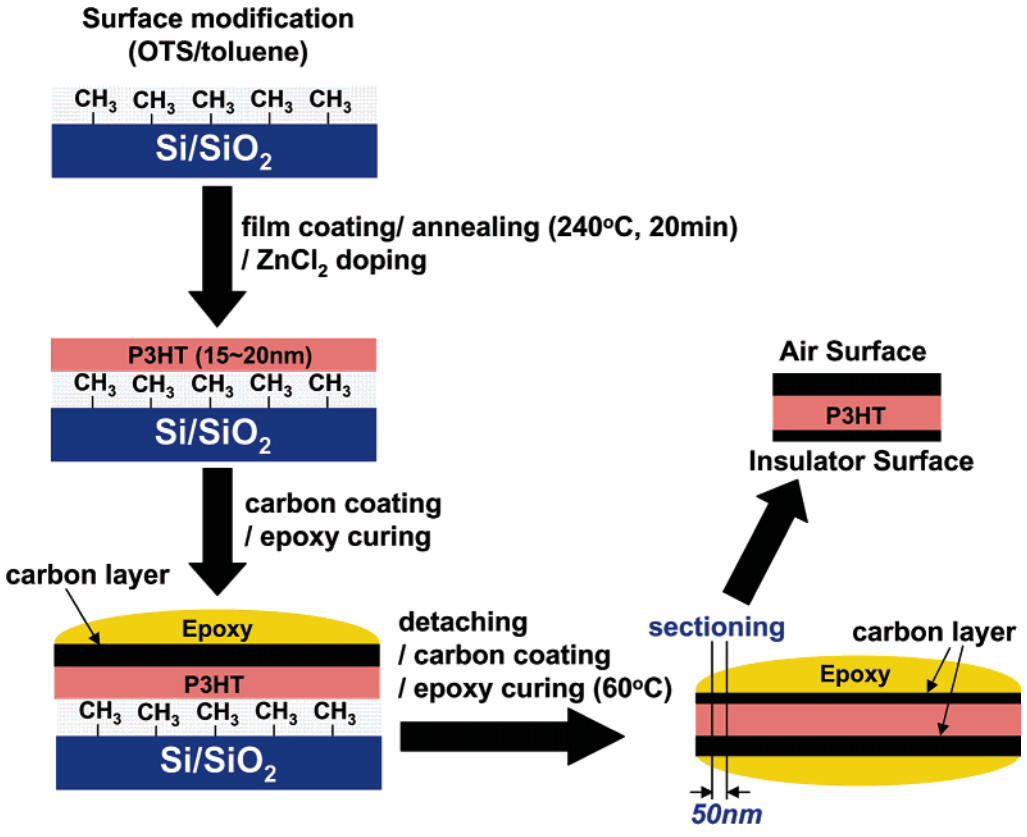

Figure 2. Overall scheme for obtaining the cross-sectional images of the layered P3HT thin films.

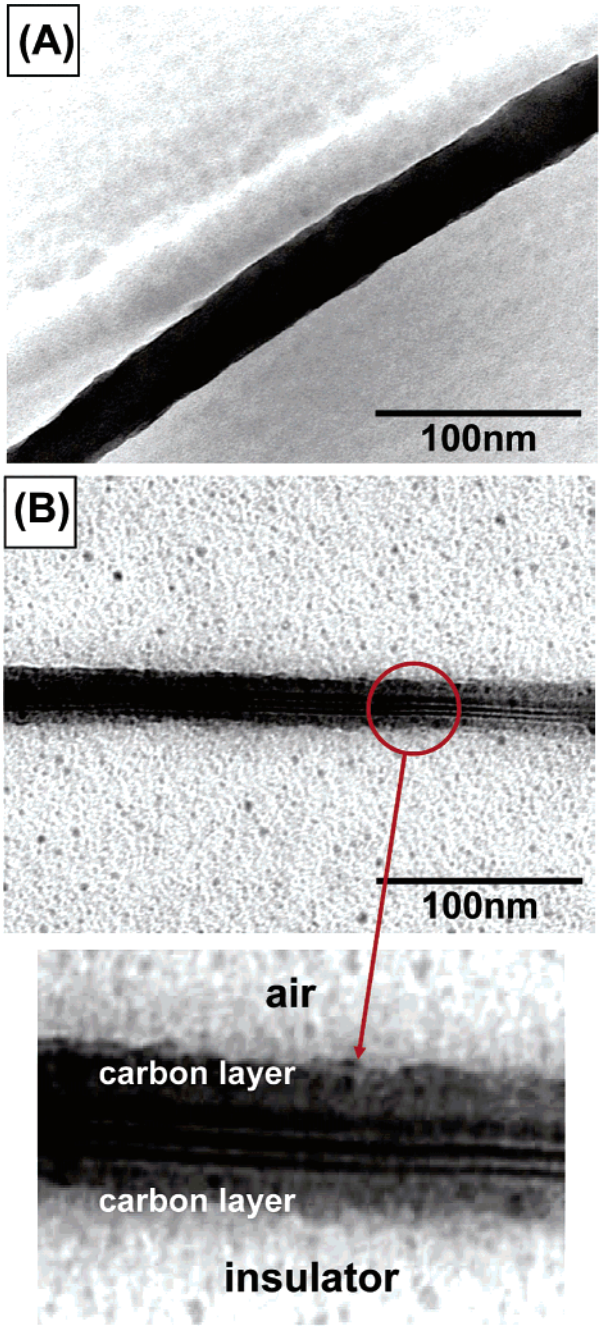

Figure 3. Cross-sectional TEM images of (A) an unannealed P3HT thin film with one-phase nanostructure and (B) an annealed P3HT thin film with layered molecular ordering.

Grazing Incidence-Angle X-ray Diffraction. The grazing-incidence X-ray diffraction measurements were performed at the 8C1and 3C2 beamline (wavelength ~ 1.54 Å) at the Pohang Accelerator Laboratory (PAL). The measurements were obtained in a scanning interval of 2θ between 3° and 32°.

Tapping Mode Atomic Force Microscopy. An atomic force microscope (Digital Instruments Multimode), operating in the tapping mode using a silicon cantilever with a spring constant of 30 N/m and a tip radius of 13 nm, was used to characterize the morphologies of the hydrophobized silicon substrates.

Results and Discussion

The overall procedure for directly visualizing the internal structures of the P3HT films is presented in Figure 2. We used a simple spin-coating method to fabricate regioregular P3HT thin films with a thickness of about 15−20 nm on hydrophobized surfaces. The resulting thin films were annealed at 240 °C (above the melting temperature of P3HT) for 20 min under argon and then slowly cooled to room temperature in order to increase the regularity of the backbone conformations. Thin layers of thickness ~40−50 nm were sectioned from the $ZnCl_2$-doped samples (1 wt % $ZnCl_2$ solution) using an ultramicrotome, and the sectioned specimens were further exposed to $ZnCl_2$ solution for 10 min.

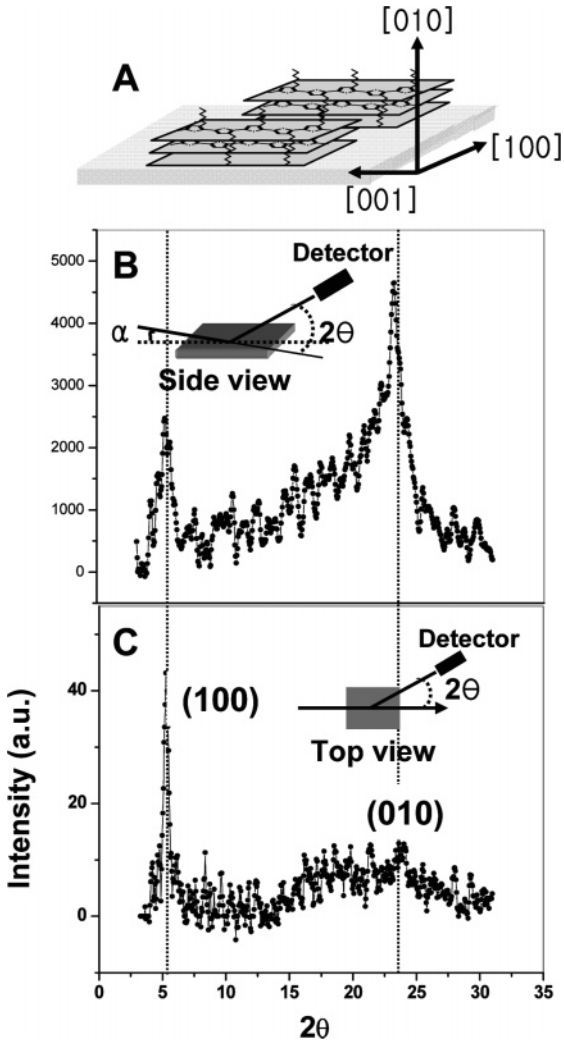

Figure 4. (A) Schematic crystallography of the nanocrystallite with respect to the hydrophobized insulator substrate, (B) out-of-plane, and (C) in-plane grazing incidence angle X-ray diffraction intensities as a function of the scattering angle 2θ for regioregular P3HT thin films crystallized on hydrophobized insulator substrates.

Layered molecular ordering was found in the annealed P3HT films prepared on hydrophobized (OTS-treated) insulator substrates, whereas the unannealed P3HT films were found to have a one-phase nanostructure, as shown in Figure 3. Since the thin films were embedded in epoxy with a carbon coating after removal from their substrates, the images were slightly undulated. Carbon layers were deposited on both sides of the films, with a thicker carbon layer deposited on the top layer to distinguish top from bottom. We conclude from the variations in contrast in the TEM image (Figure 3B) that the cross-sectioned film is composed of six layers. Layers with higher contrast (i.e., black parts) are highly doped; individual layers with high contrast and a thickness of 5 nm were observed. We speculate that these layers might be composed of fewer $\pi-\pi$ stacked P3HT chains (disordered domain) of limited size, which enables greater doping of such layers with $ZnCl_2$. Layers with

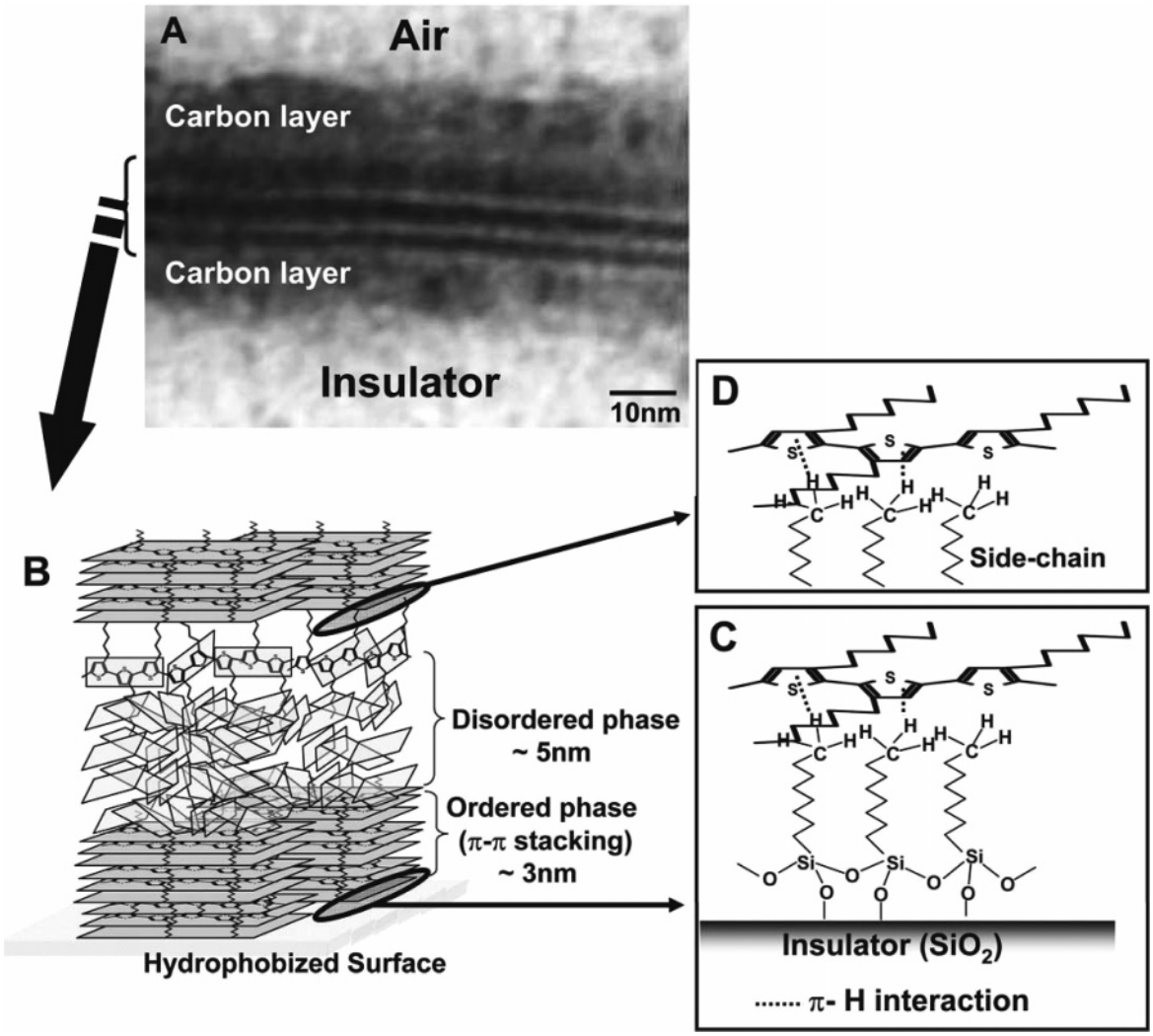

Figure 5. (A) Highly magnified cross-sectional TEM image of a P3HT thin film, (B) schematic representation of image (A), (C) schematic representation of the orientation of P3HT chains near the interface between P3HT and the hydrophobized insulator surface, and (D) schematic representation of the orientation of P3HT chains near the interface between the P3HT side chains of the disordered layer and the thienyl backbones of the next P3HT chains above the disordered layer.

lower contrast (i.e., white parts) are less doped; these are individual layers with a thickness of 3 nm, which consist of $\pi-\pi$ stacked P3HT chains (ordered domain) that inhibit doping by $ZnCl_2$. Starting from the bottom (from the thinner carbon layer), the following layers can be seen: a light layer, then a dark layer, and another dark layer at the top (under the thicker carbon layer). However, we did not observe such layered molecular ordering in unannealed films and or in a film annealed at a temperature (120 °C) below the melting temperature, at which only the side chains of P3HT are mobile (Figure 3A). Above the melting temperature, both the backbone and side chains of P3HT are mobile. A drastic change in the internal nanostructure of P3HT is observed as a result of annealing at high temperature.

Actually, as the field-effect occurs in the first few layers of the P3HT thin film, the ordering of the bottom layer on the insulator substrate is crucial. We found that the unannealed P3HT thin film consists only of a single phase, not a layered structure, indicating that disordered structure is present throughout the film; in contrast, the annealed P3HT has an ordered bottom layer (Figure 3). In a previous study,[7a] we found that heat treatment results in a field-effect mobility (0.08 $cm^2\ V^{-1}\ s^{-1}$ for face-on orientation) that is more than a factor of 8 higher than that of as-prepared samples (0.01 $cm^2\ V^{-1}\ s^{-1}$), showing the random orientation irrespective of surface characteristics.

To determine the chain orientation in the ordered domains (the white parts of Figure 3B) more precisely, synchrotron grazing-incidence X-ray diffraction (GI-XRD) measurements were carried out on the spin-coated films (thickness ~ 15 nm). By using a fixed grazing incidence angle (0.18°) that is above the critical angle for total reflection from the regioregular P3HT thin films but below the critical angle (0.23°) of the insulator (SiO_x) substrate, the scattering from the substrate was reduced relative to the scattering from the films. Figure 4A schematically shows the face-on orientation of the nanocrystalline P3HT domains with respect to the hydrophobized substrate. This face-on structure is evident from the different intensity distributions of the (100) reflections due to the lamellar layer structure (16.4 Å) and the (010) reflections due to $\pi-\pi$ interchain stacking (3.8 Å) in the out-of-plane (Figure 4B) and in-plane (Figure 4C) geometric modes. In other words, P3HT thin films fabricated on hydrophobized insulator substrates with CH_3 end groups are preferentially oriented along the (100)-axis in the plane and the (010)-axis normal to the film. This face-on orientation was found to depend strongly on the surface characteristics of the insulator substrate. However, perfect face-on orientation is not evident in Figure 4B (relatively strong (100) diffraction is present for the out-of-plane geometry) because there are a few $\pi-\pi$ stacked P3HT chains in disordered layers with slightly random orientations. In this π-conjugated system,

there are π-H interactions between the thienyl backbone bearing the π system and the H atoms (hydrogens) of the OTS−SAM end groups.[7b,9] In general, the π-H interaction is modulated as a result of changes in the electronegativity of the atom attached to hydrogen. However, unlike conventional H-bonds, this enhancement cannot be simply explained in terms of the increase in electrostatic interactions or the electronegativity of the atom bound to the π-H bonded proton. The contributions of each of the attractive (electrostatic, inductive, disperse) and repulsive exchange components of the total binding energy are important. If there is no repulsive force between the SAM end group and the thienyl backbone, the face-on conformation is energetically more favored, which is in line with the thermodynamic stability caused by the aromatic π-H interaction and the low dipole moment ($\mu\sim$ 0.2 D).[7b] We deduce that in systems without unshared electron pairs ($-CH_3$) the orientation of P3HT chains parallel to the insulator substrate (face-on structure) is the most thermodynamically stable orientation because of the π-H interactions,[7b,9] as shown in Figure 5C. Therefore, the formation of the first layer to form, the 3 nm ordered layer on the CH_3-modified substrate, is influenced by the favorable π-H interactions between the CH_3−SAM and the P3HT chains and the $\pi-\pi$ interchain stacking between P3HT chains. On top of the 3 nm ordered layer there is an ∼5 nm thick disordered layer, which presumably arises because of the limited coherent length of the ordered domains. The presence of randomly oriented P3HT chains on the surface of the disordered layer might induce π-H interactions between the side chains of the disordered layer (H) and the thienyl backbones of the P3HT chains in the next layer (π), which could result in the formation of an ordered layer on top of the disordered layer (Figure 5D).

The cross-sectional TEM and GI-XRD results demonstrate that layered molecular ordering results from the thermal annealing process and the presence of the hydrophobized insulator substrate. From these results, we conclude that the internal morphology of a regioregular P3HT thin film grown on a hydrophobized insulator substrate is as shown schematically in Figure 5B.

Conclusion

In summary, we have demonstrated through direct visualization that P3HT films on hydrophobized insulator substrates are self-organized with layered molecular ordering. Further, our GI-XRD results showed that highly oriented, nanoscopic domains composed of P3HT chains with face-on orientation were produced.

Acknowledgment. This work was supported by the POSTECH Research Program, the National Research Laboratory Program, and ERC Program (R11-2003-006-03005-0) of the MOST/KOSEF, a grant (F0004022) from Information Display R&D Center under the 21st Century Frontier R&D Program and the Regional Technology Innovation Program (RTI04-01-04) of the MOCIE, the BK21 Program of the Ministry of Education and Human Resources Development of Korea, and the Pohang Acceleratory Laboratory for providing the synchrotron radiation source at the 4C2, 3C2, and 8C1 beamlines used in this study.

References and Notes

(1) (a) Tessler, N.; Harrison, N. T.; Friend, R. H. *Adv. Mater.* **1998**, *10*, 64. (b) Huitema, H. E. A.; Gelinck, G. H.; van der Putten, J. B. P. H.; Kuijk, K. E.; Hart, C. M.; Cantatore, E.; Herwig, P. T.; van Breemen, A. J. M. M.; deLeeuw, D. M. *Nature (London)* **2001**, *414*, 599. (c) Horowitz, G. *Adv. Mater.* **1998**, *10*, 365. (d) Kraft, A.; Grimsdale, A. C.; Holmes, A. B. *Angew. Chem., Int. Ed.* **1998**, *37*, 402. (e) Cao, Y.; Parker, I. D.; Yu, G.; Zhang, C.; Heeger, A. J. *Nature (London)* **1999**, *397*, 414. (f) Jenekhe, S. A.; Yi, S. *Appl. Phys. Lett.* **2000**, *77*, 2635. (g) Huynh, W. U.; Dittmer, J. J.; Alivisatos, A. P. *Science* **2002**, *295*, 2425. (i) Brabec, C. J.; Sariciftci, N. S.; Hummelen, J. C. *Adv. Funct. Mater.* **2001**, *11*, 15.

(2) (a) Bao, Z.; Dodabalapur, A.; Lovinger, A. J. *Appl. Phys. Lett.* **1996**, *69*, 4108. (b) Lovinger, A. J.; Rothberg, L. J. *J. Mater. Res.* **1996**, *11*, 1581. (c) Garnier, F.; Hajlaoui, R.; Yassar, A.; Srivastava, P. *Science* **1994**, *265*, 1684.

(3) (a) Sirringhaus, H.; Tessler, N.; Friend, R. H. *Science* **1998**, *280*, 1741. (b) Österbacka, R.; An, C. P.; Jiang, X. M.; Vardeny, Z. V. *Science* **2000**, *287*, 839. (c) Sirringhaus, H.; Brown, P. J.; Friend, R. H.; Nielsen, M. M.; Bechgaard, K.; Langeveld-Voss, B. M. W.; Spiering, A. J. H.; Janssen, R. A. J.; Meijer, E. W.; Herwig, P.; de Leeuw, D. M. *Nature (London)* **1999**, *401*, 685. (d) Stutzmann, N.; Friend, R. H.; Sirringhaus, H. *Science* **2003**, *299*, 1881. (e) Drury, C. J.; Mutsaers, C. M. J.; Hart, C. M.; Matters, M.; deLeeuw, D. M. *Appl. Phys. Lett.* **1998**, *73*, 108. (f) Dodabalapur, A. *Appl. Phys. Lett.* **1998**, *73*, 142. (g) Dimitrakopoulos, C. D.; Malenfant, P. R. L. *Adv. Mater.* **2002**, *14*, 99. (h) Abdel-Mottaleb, M. M. S.; Götz, G.; Kilickiran, P.; Bäuerle, P.; Mena-Osteritz, E. *Langmuir* **2006**, *22*, 1443.

(4) (a) Seshadri, K.; Frisbie, C. D. *Appl. Phys. Lett.* **2001**, *78*, 993. (b) Kim, D. H.; Han, J. T.; Park, Y. D.; Jang, Y.; Cho, J. H.; Hwang, M.; Cho, K. *Adv. Mater.* **2006**, *18*, 719.

(5) (a) Chen, T. A.; Wu, X.; Rieke, R. D. *J. Am. Chem. Soc.* **1995**, *117*, 233. (b) Prosa, T. J.; Winokur, M. J.; McCullough, R. D. *Macromolecules* **1996**, *29*, 3654. (c) McCullough, R. D. *Adv. Mater.* **1998**, *10*, 93.

(6) (a) Sirringhaus, H.; Brown, P. J.; Friend, R. H.; Nielsen, M. M.; Bechgaard, K.; Langeveld-Voss, B. M. W.; Spiering, A. J. H.; Janssen, R. A. J.; Meijer, E. W. *Synth. Met.* **2000**, *111−112*, 129. (b) Kline, R. J.; McGehee, M. D.; Kadnikova, E. N.; Liu, J.; Fréchet, J. M. J. *Adv. Mater.* **2003**, *15*, 1519. (c) Kline, R. J.; McGehee, M. D.; Toney, M. F. *Nat. Mater.* **2006**, *5*, 222. (d) Kline, R. J.; McGehee, M. D.; Kadnikova, E. N.; Liu, J.; Fréchet, J. M. J.; Toney, M. F. *Macromolecules* **2005**, *38*, 3312. (e) Babel, A.; Jenekhe, S. A. *J. Phys. Chem. B* **2003**, *107*, 1749. (f) Babel, A.; Jenekhe, S. A. *Synth. Met.* **2005**, *148*, 169. (g) Yang, H.; Shin, T. J.; Yang, L.; Cho, K.; Ryu, C. Y.; Bao, Z. *Adv. Funct. Mater.* **2005**, *15*, 671. (h) Sandberg, H. G. O.; Frey, G. L.; Shkunov, M. N.; Sirringhaus, H.; Friend, R. H. *Langmuir* **2002**, *18*, 10176. (i) Apperloo, J. J.; Janssen, R. A. J.; Nielsen, M. M.; Bechgaard, K. *Adv. Mater.* **2000**, *12*, 1594. (j) Chang, J.-F.; Sun, B.; Breiby, D. W.; Nielsen, M. M.; Solling, T. I.; Giles, M.; McCulloch, I.; Sirringhaus, H. *Chem. Mater.* **2004**, *16*, 4772. (k) Liu, J.; Sheina, E.; Kowalewski, T.; McCullough, R. D. *Angew. Chem., Int. Ed.* **2002**, *41*, 329. (l) Aasmundtveit, K. E.; Samuelsen, E. J.; Guldstein, M.; Steinsland, C.; Flornes, O.; Fagermo, C.; Seeberg, T. M.; Petterson, L. A. A.; Inganäs, O.; Feidenhans'l, R.; Ferrer, S. *Macromolecules* **2000**, *33*, 3120.

(7) (a) Kim, D. H.; Park, Y. D.; Jang, Y. S.; Yang, H. C.; Kim, Y. H.; Han, J. I.; Moon, D. G.; Park, S.; Chang, T.; Chang, C.; Joo, M.; Ryu, C. Y.; Cho, K. *Adv. Funct. Mater.* **2005**, *15*, 77. (b) Kim, D. H.; Jang, Y. S.; Park, Y. D.; Cho, K. *Langmuir* **2005**, *21*, 3203.

(8) Trznadel, M.; Pron, A.; Zagorska, M.; Chrzaszcz, R.; Pielichowski, J. *Macromolecules* **1998**, *31*, 5051.

(9) Tarakeshwar, P.; Choi, H. S.; Kim, K. S. *J. Am. Chem. Soc.* **2001**, *123*, 3323.

MA060427B